

RINOPOLYCRETE - TOWARDS A CEMENT-FREE AND FULLY RECYCLED CONCRETE



PROJECTO FCT

PTDC/ECI-COM/29196/2017

**Recycled inorganic polymer concrete - Towards a cement-free and fully recycled concrete
(RInoPolyCrete)**

Task 4 - Report 2

Environmental impact and technical performance of recycled concrete containing municipal incinerated bottom ash

September, 2022
Financiamento FCT/POCI



Governo da República Portuguesa



União Europeia FEDER

FCT Fundação para a Ciência e a Tecnologia
MINISTÉRIO DA CIÊNCIA E DO ENSINO SUPERIOR Portugal

TABLE OF CONTENTS

1	INTRODUCTION	1
2	METHODOLOGY.....	1
3	MATERIALS AND METHODS.....	4
3.1	PREPARING MIBA FOR TREATMENT.....	4
3.1.1	<i>Collection and sampling</i>	<i>4</i>
3.1.2	<i>Milling.....</i>	<i>5</i>
3.1.2.1	Preparation MIBA before grinding	5
3.1.2.2	Grinding in the Los Angeles abrasion machine.....	6
3.1.2.3	Crushing in the cylinder mill	6
3.1.2.4	Crushing in the ball mill.....	7
3.1.2.5	Sieving.....	7
3.2	TREATMENT.....	8
3.2.1	<i>Aluminium treatment manually.....</i>	<i>8</i>
3.2.2	<i>Chemical treatment.....</i>	<i>9</i>
3.2.2.1	Test setup calibration.....	9
3.2.2.2	Quantification of metallic aluminium in MIBA	10
3.3	EXPERIMENTAL CAMPAIGN	11
3.3.1	<i>Materials.....</i>	<i>11</i>
3.3.1.1	Aggregates.....	11
3.3.1.1	Cement.....	14
3.3.1.1	Fly ash	14
3.3.1.1	Water and superplasticizer.....	15
3.3.2	<i>Concrete formulation.....</i>	<i>15</i>
3.3.3	<i>Production and curing of the concrete</i>	<i>16</i>
3.3.4	<i>Testing methods</i>	<i>19</i>
3.4	RESULTS AND DISCUSSION	21
3.4.1	<i>Composition of MIBA.....</i>	<i>21</i>
3.4.2	<i>Aggregate characterization</i>	<i>23</i>
3.4.3	<i>Quantification of metallic aluminium in MIBA.....</i>	<i>26</i>
3.4.4	<i>Compressive strength</i>	<i>29</i>
4	CONCLUSIONS	32
	REFERENCES.....	34

ACRONYMS

MIBA	Municipal solid waste incinerator bottom ash
M	Molarity
NaOH	Sodium hydroxide
SCM	Supplementary cementitious material
W	Water
WA	Water absorption

1 Introduction

The demand of the extraction of natural resources has significantly increased due to the amount of concrete used in the construction industry, which has a significant impact on the emissions released into the biosphere and energy consumption. Using by-products as a SCM in concrete can be a solution to reduce the mentioned impacts. There are many waste materials (e.g. municipal solid waste incinerator bottom ash - MIBA) that can be used in concrete. However, some must be treated before their use in concrete.

There are several economic and sustainability benefits to using MIBA as an SCM in concrete. However, its use also involves addressing challenges that most "traditional" SCMs do not have. Most of these SCM do not have aluminium, which negatively affects the performance of concrete, whereas the chemical composition of MIBA mainly depends on its original waste materials (including aluminium bottle caps, cans, etc.).

The presence of metallic aluminium is a problem to consider in MIBA, because it reacts with water and some cement hydration products and produces hydrogen gas as a result. This results in expansion with negative effects on strength and durability. There are some studies looking for new and feasible techniques in dealing with this problem by accelerating the reaction between aluminium and water with alkali materials before using MIBA (Alderete et al., 2021). Some of the proposed methods are effective, but they are either expensive to perform or not adequate for mass production. Thus, this report presents a description of the preparation and treatment of municipal solid waste incinerator bottom ash (MIBA) with a method that can overcome the aforementioned issue. Moreover, it explains the procedures adopted to make the experimental campaign and presents results related to compressive strength test of all mixes.

2 Methodology

As shown in Figure 1, this work followed a certain methodology that can be divided into four distinct steps (i-iii). Figure 2 shows all procedures and the steps that were followed throughout the experimental campaign:

(i) The first one explains the procedures required before producing concrete such as preparing MIBA before using it as a SCM, which includes: collecting and sampling, grinding, and sieving processes (Figure 2);

(ii) The second step established the methods for treating MIBA, starting with the manual aluminium treatment, then chemical treatment of MIBA, and finally checking and improving the process that was followed in the test. These steps are essential for extracting and recycling aluminium within MIBA (Figure 3);

(iii) The third step explains the experimental work and the steps applied in the laboratory and procedures of casting mixes of concrete (Figure 3);

(iv) The last step is the inclusion of treated and untreated MIBA in concrete mixes, which refers to the summary and explanation the results (outputs) of the tests that did during the work.

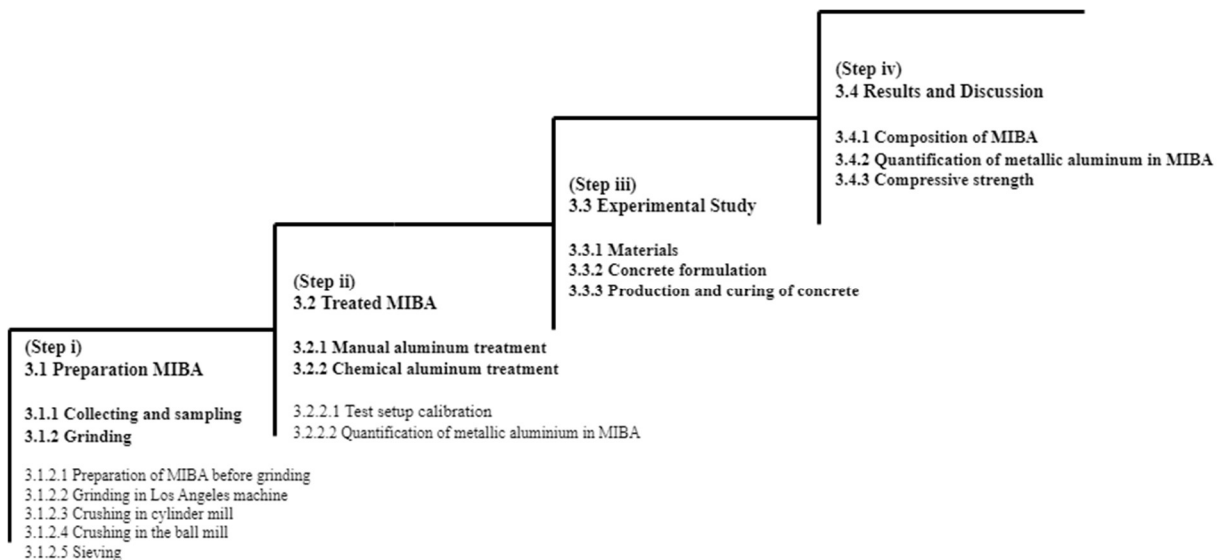


Figure 1 - Methodology of work

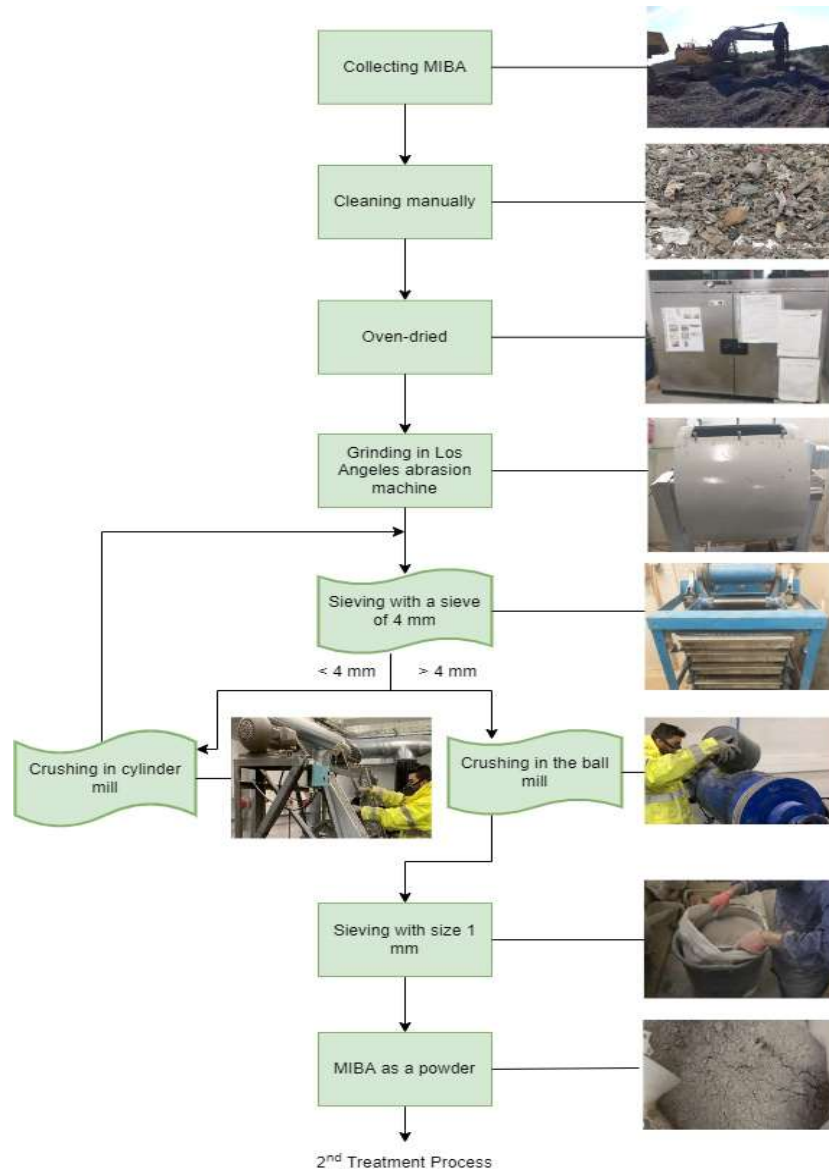


Figure 2 - The sequence of procedures from MIBA extraction to practical application

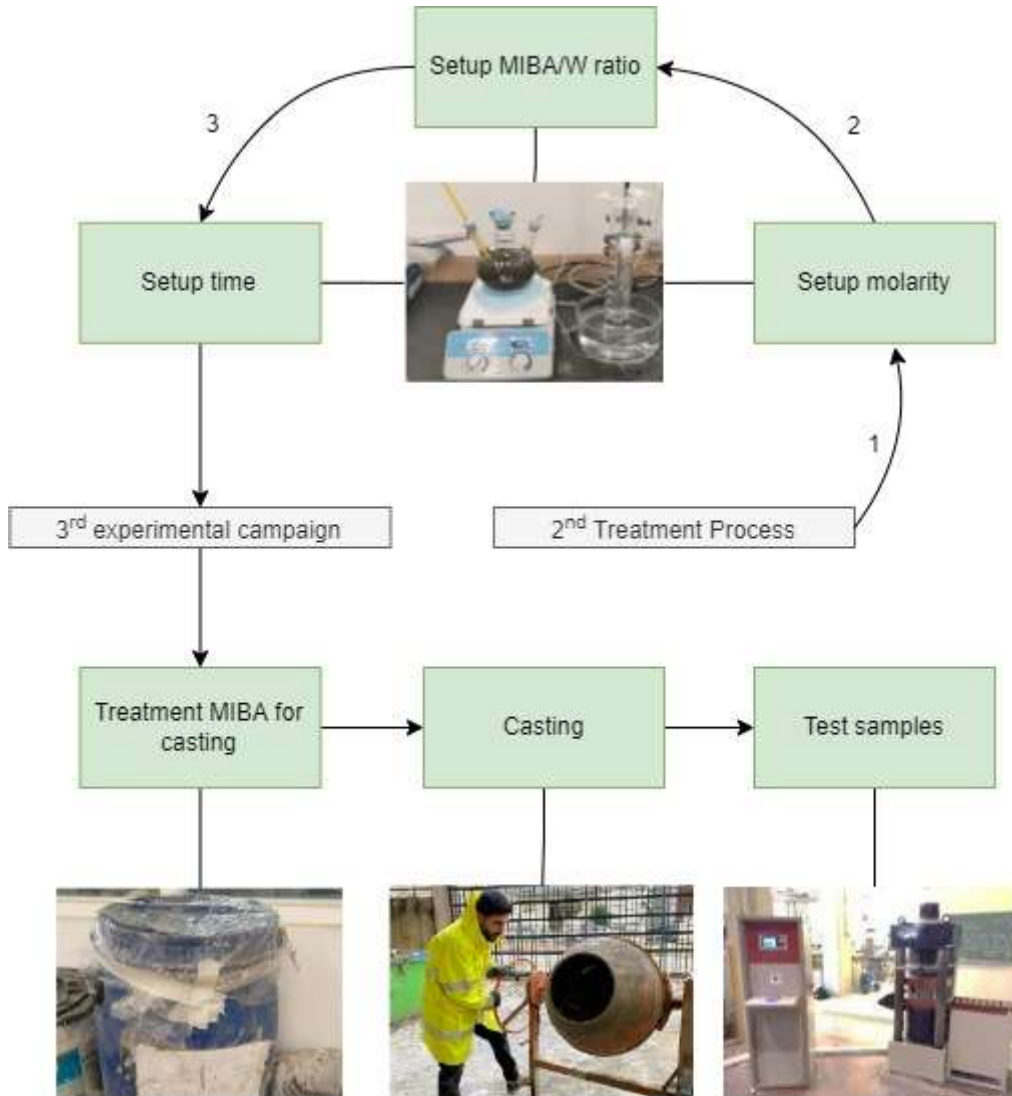


Figure 3 - The sequence of procedures of MIBA treatment and experimental campaign

3 Materials and methods

3.1 Preparing MIBA for treatment

3.1.1 Collection and sampling

MIBA was collected in the Valorsul facility (Lisbon, Portugal) in January, 2019. A stationary sampling of the pile was done using a long-arm excavator, which made six perforations at different depths, distributed evenly throughout the slope (Figure 4).



Figure 4 - MIBA stacks separated by monthly production (a); MIBA sampling (b)

The MIBA was homogenised by depositing it onto a flat surface, churning it continuously using an excavator (Figure 5). Finally, a representative sample was taken from the stockpile and carried in large bags to the lab.



Figure 5 - Homogenization of MIBA

3.1.2 Milling

3.1.2.1 Preparation MIBA before grinding

The MIBA samples were dried at 105 °C until constant mass was reached. The mass was considered constant when, in two consecutive weightings, separated by one hour, it did not vary by more than 0.1% (Figure 6a). After drying, the MIBA was subjected to a manual triage, in which plastic, wooden or metallic particles were removed (Figure 6b), as they would have a negative effect on the performance of concrete containing MIBA.

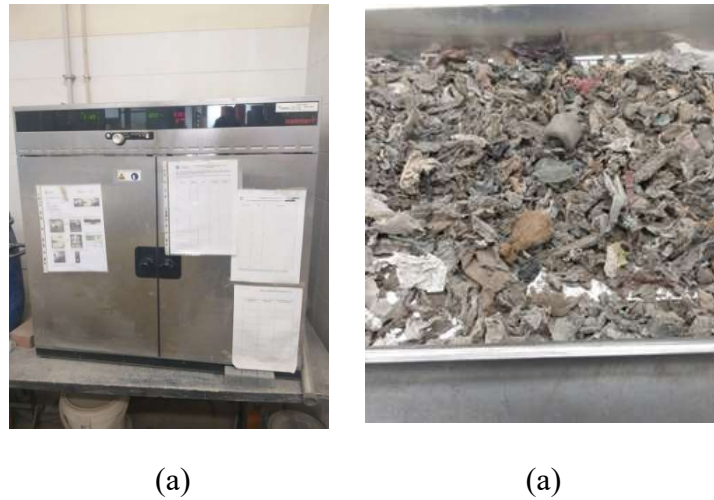


Figure 6 - Dry in oven(a); Material after manual triage (b)

3.1.2.2 Grinding in the Los Angeles abrasion machine

In the Los Angeles abrasion machine, 20 kg of the material resulting from the previous step were ground for 30 minutes using an abrasive load of 12.30 kg of steel (31 steel balls). In order to isolate the bigger particles for further size reduction, the resulting MIBA was screened using a 4-mm sieve (Figure 7).

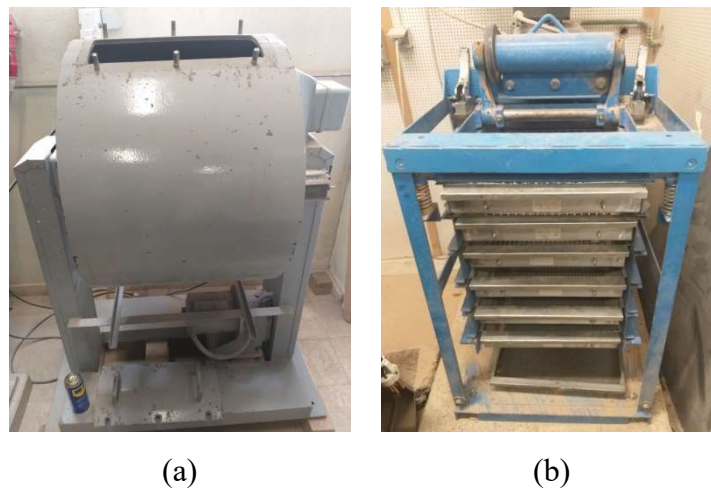


Figure 7 - Los Angeles machine (a); Sieves (b)

3.1.2.3 Crushing in the cylinder mill

In order to use particles larger than 4 mm resulting from the previous process, these were fed into a cylinder mill. Only afterwards were the resulting particles placed in the ball milling machines to guarantee that the product was similar to cement in terms of particles distribution (Figure 8).



(a)



(b)

Figure 8 - Cylinder milling machine (a); Ball milling machine (b)

3.1.2.4 *Crushing in the ball mill*

Approximately 20 kg of MIBA were ground in a ball mill for two hours to generate a powdery product with an average particle size comparable to that of cement. This was done by employing an abrasive load of 56 kg of steel balls with diameters ranging from around 5 cm to 30 cm.



Figure 9 - MIBA sieving with 1 mm sieve (a); Container for preventing the humidity of MIBA (b)

3.1.2.5 *Sieving*

The last part of the procedure to prepare milled MIBA is sieving it using a 1-mm sieve to remove the larger particles that endured the milling process, many of which were aluminium particles. Afterwards, the material was stored in a sealed container to avoid moisture (Figure 9).

3.2 Treatment

3.2.1 Aluminium treatment manually

The final product of grinding MIBA was sieved using a sieve that size 1 mm. This fraction includes greyish metallic flake-like particles, with high aluminium content that were left without grinding and held during sieving on the 1 mm sieve. The aluminium fractions collected from the previous step could then be recycled by melting them in a 700-800 °C oven to produce pure aluminium. As a result, aluminium can be extracted from MIBA to be used. The advantage in this way is to manually reduce aluminium presence within MIBA, as well as recycle the aluminium obtained from MIBA (Figure 10).



(a)



(b)



(c)



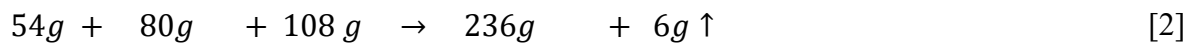
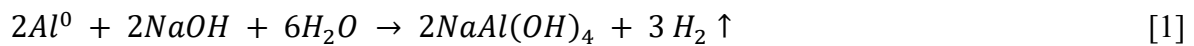
(d)

Figure 10 - 1 mm sieve used on MIBA in the first stage (a); Aluminium fractions prior to melting (b); Aluminium fractions placed in 700°C oven (c); Aluminium alloy (d).

3.2.2 Chemical treatment

3.2.2.1 Test setup calibration

As stated, MIBA may contain a considerable amount of aluminium. This metal can react with the OH⁻-rich solutions (fresh cement paste) and, as a result, sodium aluminate and a sizeable amount of hydrogen gas will be produced. The stoichiometric quantities (atomic and molecular weights) of the mentioned reaction can be seen, in grams, in Eq. 1, Eq. 2, and Eq. 3. Each gram of aluminium produces 0.11 g of H₂↑.



$$g H_2 \uparrow = 1 g Al^0 \times \frac{6 g H_2 \uparrow}{54 g Al^0} = 0.11 g \quad [3]$$

In order to quantify the amount of Al present in MIBA and H₂ produced from it, the following tools were used in the experiment campaign:

- Volumetric flask;
- Test tube;
- A plastic pipe connected to the volumetric flask with the test tube (Figure 11).

In order to support the theoretical formulas given in Eq. 1-3, and calibrate the experimental tools, the following procedure was performed before measuring the amount of Al in MIBA. First, the reaction of 0.1 g of aluminium metal with a 2.5 M NaOH solution was experimentally measured to find the released hydrogen gas according to the evicted volume of water from an inverted test tube connected to the volumetric flask by a plastic pipe. Theoretically, 0.1 g of aluminium metal produces 143.603 ml of hydrogen gas). Three tests were made to determine the mean and the standard deviation. The reaction between NaOH and water produced a temperature of 43 °C.

As shown in Eq. 4 and Eq. 5, the volume of released hydrogen can be calculated by using mass of hydrogen produced by each gram of aluminium and its density. The density of released hydrogen is 0.0766 kg /m³ at 43 °C and 1 atm. pressure. This leads to the fact that one gram of aluminium metal produces 1.436 litres of hydrogen.



Figure 11 - Tools used to quantify the amount of Al

$$v = \frac{m}{\rho} \quad [4]$$

$$v_{H_2} = \frac{0,11}{0.0000766} = 1436.03 \text{ ml} \quad [5]$$

3.2.2.2 Quantification of metallic aluminium in MIBA

Using the same test setup mentioned in the previous section, it was possible to quantify the amount of metallic aluminium in MIBA (Figure 11). Thus, the test was carried out with 15 g of MIBA and 800 ml of a 2.5M NaOH solution in order to quantify the volume of hydrogen produced and subsequently the amount of metallic aluminium in grams per kg of MIBA. The results are presented in (Table 1). Using the density property, where density is equal to mass divided by volume, it was possible to conclude the mass of metallic aluminium in MIBA.

Table 1 - Hydrogen quantity produced from reacting sodium hydroxide with aluminium

Initial volume (ml)	Final volume (ml)	Expected volume (ml)
90	222	132
225	362	137
120	250	130
Media	-	133
SD	-	5,03
Error	-	8%

Using the stoichiometric amounts, the amount of metallic aluminium that produces this amount of hydrogen was determined (Eq. 6 and 7). In order to obtain an optimum treatment procedure, several parameters were changed. The value of molarity was chosen considering sustainability and economic reasons for the treatment of MIBA, which started at the minimum, and increase

it to find the best value that achieves the treatment. namely, water content (50 ml and 800 ml), molarity (0.25, 1, 1.5, 2.5 and 10 M), type of MIBA (ground and unprocessed), MIBA content (15 g and 25 g). In the first test, a molarity of 0.25 M and a MIBA/water (MIBA/W) ratio equal to 0.02 were used. In following tests, the molarity was increased to ascertain the amount of aluminium in MIBA without risk of having unreacted particles. Additionally, to better replicate the actual conditions at which the MIBA will be treated, a MIBA/W ratio equal to 0.50 was used and the molarity was reduced to 0, 0.1 and 0.25 to minimize the use of NaOH.

$$m = v * \alpha \quad [6]$$

$$g Al^{\circ} = 0.00485 g H_2 \uparrow \times \frac{54 g Al^{\circ}}{6 g H_2 \uparrow} = 0.04365 g Al^{\circ} \quad [7]$$

3.3 Experimental campaign

The physical and chemical properties of the NA and RCA, OPC, FA, and MIBA are discussed in this chapter. For each test, the mix design, concrete batch mixing technique, moulding, curing, preparation, and testing of concrete samples are also specified. The numerous tests in the fresh and hardened stage of the concrete samples are also described in depth and carried out in the Construction Laboratory of the Instituto Superior Técnico (IST)/Civil Engineering, Architecture, and Georesources Department in Lisbon, Portugal.

3.3.1 Materials

3.3.1.1 Aggregates

Large polypropylene bags carrying NA arrived at the IST - Construction Laboratory. By crushing the source concrete that was ordered from an outside company, RCA was created at the IST Construction Laboratory. They were oven-dried for 5-7 hours to totally remove their moisture content in order to maintain their qualities throughout the trial period. A moisture analyser was then used to determine the aggregates' moisture content to ensure that they were 100 percent dry. The aggregates were sealed in plastic containers once they were completely dry to prevent them from absorbing moisture during the experimental campaign. Two varieties of natural silica sand were used in this study, coarse and fine, which were obtained from suppliers in Sesimbra and Seixal, respectively. Silica sands in their natural state can be seen in Figure

12. The fine sand, with a nominal size of 0/2 mm, is a washed sand without organic matter and clay content and has a uniform, slightly yellowish look. The sand has small, largely uniform grains that range in shape from sub-spherical to somewhat angular. It is primarily made up of silica minerals, with some feldspar grains, according to its mineralogical makeup. The coarse sand was washed, yellowish, free of organic matter, and contains little clay. Its nominal size was of 0/4 mm. The sand had unevenly sized and shaped grains, ranging from spherical to angular. Its main constituents in terms of mineralogical composition were quartz and feldspar grains, with the latter showing minor colour variation. The sizes of three crushed limestone aggregates - rice grain, fine gravel, and coarse gravel - were varied (Figure 13). The supplier for the crushed limestone aggregates was in Sesimbra. The Lisbon area commonly employs these coarse aggregates.



Figure 12 - Sieved fine (a) and coarse river sand (b)

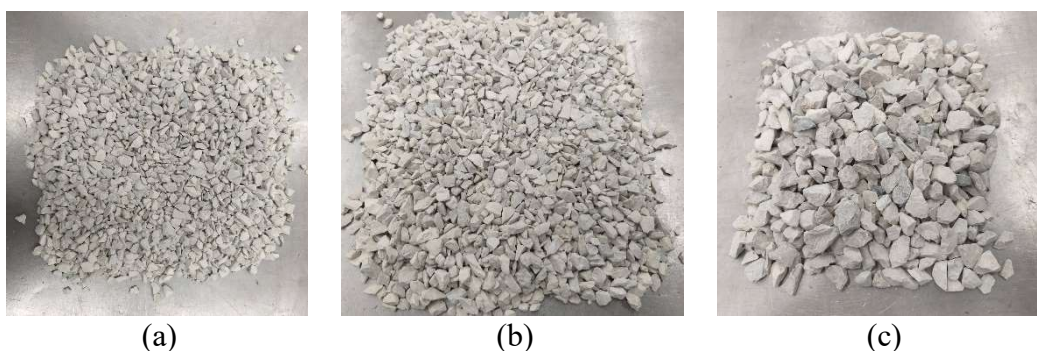


Figure 13 - Sieved crushed limestone aggregates: rice grain (a); fine gravel (b); and coarse gravel (c)

The coarse RCA were prepared in the IST laboratory. The source concrete was ordered from a concrete company based on the following requirements:

- Strength class: C30/37;
- Cement content 350 kg/m³;

- w/b: 0.45;
- Exposure class: XC2(P);
- Slump: S3 (100 - 150 mm);
- Type of cement: CEM II/A-L (Class 42,5 R, in 50 kg bags, from the Outão, Setúbal, plant);
- Maximum size of aggregates: 22.4 mm.

The mechanical strength of the ready-mixed concrete was examined at the ages of 28 and 91 days. 11 cubes of the source concrete were cast and cured in the wet chamber. After that, the concrete cubes were tested at the days mentioned previously. The results showed that the actual compressive strength of the source concrete was 42.02 MPa and 50.3 MPa (average $f_{cm,cube}$) at 28 and 91 days, respectively. The average strength of the concrete cubes complied with the target strength (C30/37). 2.5 m³ of ready concrete mix was cast (Figure 14) into three sets of wooden formwork (Figure 14a, b). After casting, they were covered with a plastic sheet to prevent water evaporation.

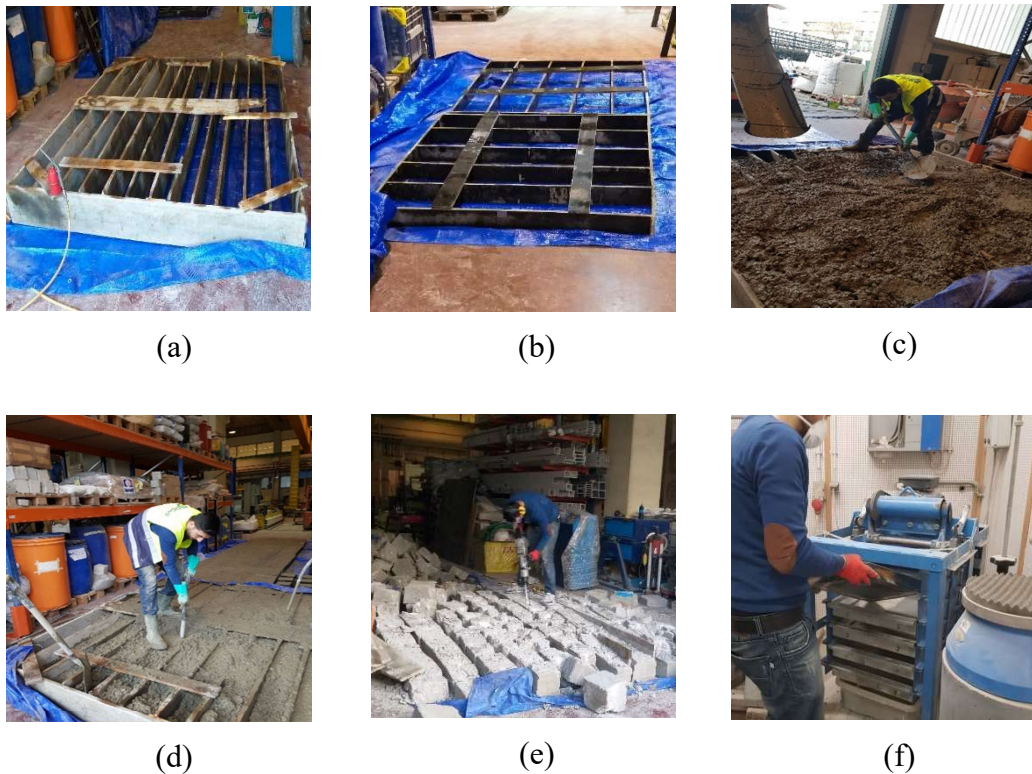


Figure 14 - Casting process of the source concrete and producing RCA; Wooden formwork(a)&(b); Casting (c); Vibrating the source concrete (d); Dividing source concrete in blocks (e); and sieving machine (f)

Concrete was demoulded in the next day and manually cut into smaller concrete blocks (Figure 14e) to be handled afterwards. At 28 days, the concrete pieces were crushed with the jaw crusher machine in conjunction with a vertical shaft impact crusher with a rotation speed of 5.73 Hz. The opening of the jaw's crusher was adjusted based on the required quantity of each size of coarse RCA. After the aforementioned process, RCA were separated and divided in five different sieves (Figure 14f) in order to obtain these sizes of coarse RCA: 4-5.6 mm, 5.6-8 mm, 8-11.2 mm, 11.2-16 mm, and 16-22.4 mm (Figure 15).



Figure 15 - Different sizes of the fine and coarse RCA

3.3.1.1 Cement

OPC type CEM I 42.5 R, complying with EN 197-1, was used to produce all concrete mixes. It is basically made of clinker (minimum content of 95%). The cement was supplied by SECIL. The chemical and physical parameters are shown briefly in Table 2.

3.3.1.1 Fly ash

FA with low calcium concentration was used. According to ASTM C618-12a (2012) and CSA-A23 (1982), whose comparable European standards are EN 450 and EN 12620, the FA was categorized as type F coal FA. The chemical and physical characteristics of the FA employed

in this study are summarized in Table 3. The results show that the particles of FA are significantly smaller than cement particles.

Table 2 - Physical, chemical, and mechanical properties of cement

Component	Results	Properties	Results
CaO (%)	63.48	Loss on ignition (%)	2.42
SiO ₂ (%)	19.49	Insoluble residue (%)	1.18
Al ₂ O ₃ (%)	5.02	Density (g/cm ³)	3.05
Fe ₂ O ₃ (%)	3.32	Initial setting (min)	161.11
MgO (%)	1.26	Final setting (min)	231.67
SO ₃ (%)	3.26	Flexural strength - 2d (MPa)	5.71
CaO (L)(%)	1.28	Flexural strength - 7d (MPa)	8.46
Cl- (%)	0.04	Flexural strength - 28d (MPa)	10.12
K ₂ O (%)	0.56	Compressive strength - 2d (MPa)	29.5
Na ₂ O (%)	0.15	Compressive strength - 7d (MPa)	45.22
C ₃ S (%)	57.67	Compressive strength - 28d (MPa)	57.69
C ₂ S (%)	16.49	Blaine specific surface (cm ² /g)	3711.78
C ₃ A (%)	4.32	Residue on the 45 μm sieve (%)	6.19
C ₄ AF (%)	11.19	Expansion (mm)	0

Table 3 - Physical and chemical properties of FA (provided by the supplier)

Chemical composition (%)									Physical properties					
LoI	SiO ₂	Al ₂ O ₃	Fe ₂ O ₃	CaO	MgO	SO ₃	Na ₂ O	K ₂ O	Sieve analysis (retained %)					Density (kg/m ³)
									200 μm	90 μm	63 μm	45 μm	32 μm	
3.8	57.8	20.9	7.4	3.6	1.0	0.6	1.0	1.7	0.21	2.92	7.82	14.42	22.48	2,300.0

3.3.1.1 Water and superplasticizer

All of the mixes contained drinking (tap) water from the public supply system. The superplasticizer used in mixes was Sika (ViscoCrete)-3011 (Figure 16d).

3.3.2 Concrete formulation

As shown in Table 4, in the two mix families (0% coarse RCA and 100% coarse RCA), the coarse NA were replaced with coarse RCA at 0% and 100% respectively. For each of these two families, three incorporation levels (20%, 33% and 55%) of untreated MIBA were used. The design criteria were:

- The target strength of the reference concrete (M1) was designed to be class C30/37 MPa (EN 1992-1-1, 2004);

- The percentage of superplasticizer was calibrated in order to maintain the slump approximately constant (125 ± 25 mm) in all mixes. w/b was fixed at 0.5 according to standard (EN 197-1, 2000);
- NA were replaced with RCA on the basis of absolute volume replacement method. The replacement of MIBA (20%, 35%, and 55%) was made by the total binder's mass (300 kg/m^3);
- Moreover, the mass and volume of the aggregates for each sieve size were chosen according to the Faury's method.

Table 4 - Incorporation ratios of treated MIBA, FA and RCA in each concrete mix

Aggregate		FA (%)				MIBA (%)			MIBA (%) + FA (%)		
		0	20%	35%	55%	20%	35%	55%	10%+10%	17.5%+17.5%	27.5%+27.5%
NA	100%	Ref.	FA20NA	FA35NA	FA55NA	TM20NA	TM35NA	TM55NA	TM10FA10NA	TM17.5FA17.5NA	TM27.5FA27.5NA
Coarse RA	100%	RAC100	-	-	-	TM20RA	TM35RA	TM55RA	-	-	-

Table 5 - Incorporation ratios of untreated MIBA, FA and RCA in each concrete mix

Aggregate		U.T.MIBA (%)		
		20%	35%	55%
NA	100%	UTM20NA	UTM35NA	UTM55NA
Coarse RA	100%	UTM20RA	UTM35RA	UTM55RA

3.3.3 Production and curing of the concrete

Concrete batches were produced using a 70-litre-capacity mixer with variable inclination as shown in Figure 16. According to the mix composition detailed in Table 6, all components including aggregates were weighed. All tools were pre-wetted before concrete production (concrete mixer, shovel, slump cone, and its board, trowel, and fresh density container). The aggregates were placed first in the mixer. Afterwards, these were blended with 2/3 of the mixing water for 6 minutes to ensure a considerably degree of saturation, with additional 4 minutes of mixing after adding the cement and the remaining water (1/3) and SP.



(a)



(b)



(c)



(d)



(e)

Figure 16 - Moulding concrete samples: Preparing moulds before filling (a); Oil-coated moulds after filling with concrete (b); Horizontal concrete mixer (c); Superplasticizer used in mixes (d); Concrete table saw (e)

Table 6 - Composition for 1 m³ of concrete

Mixes	M1 Ref.	M2 FA20NA	M3 FA35NA	M4 FA55NA	M5 RCA100	M6 TM20NA	M7 TM35NA	M8 TM55NA	M9 UTM20NA	M10 UTM35NA
FA	0.00	60.00	105.00	165.00	0.00	0.00	0.00	0.00	0.00	0.00
MIBA	0.00	0.00	0.00	0.00	0.00	60.00	105.00	165.00	60.00	105.00
Cement	300.00	240.00	195.00	135.00	300.00	240.00	195.00	135.00	240.00	195.00
Water	160.77	160.69	160.63	160.55	196.31	160.73	160.63	160.55	160.73	160.63
Fine sand 0/1	303.39	301.19	299.54	297.34	303.39	302.22	299.54	297.34	302.22	299.54
Coarse sand 0/4	591.99	587.70	584.48	580.19	591.99	589.71	584.48	580.19	589.71	584.48
Sand-Gravel 2/5.6	102.38	101.64	101.08	100.34	0.00	101.98	101.08	100.34	101.98	101.08
Fine gravel 5.6/11.2	250.37	248.55	247.19	245.38	0.00	249.40	247.19	245.38	249.40	247.19
Coarse gravel 10/20	662.91	658.11	654.50	649.70	0.00	660.35	654.50	649.70	660.35	654.50
4 - 5.6	0.00	0.00	0.00	0.00	93.65	0.00	0.00	0.00	0.00	0.00
5.6 - 8	0.00	0.00	0.00	0.00	106.40	0.00	0.00	0.00	0.00	0.00
8 - 11.2	0.00	0.00	0.00	0.00	107.71	0.00	0.00	0.00	0.00	0.00
11.2 - 16	0.00	0.00	0.00	0.00	277.36	0.00	0.00	0.00	0.00	0.00
16 - 22.4	0.00	0.00	0.00	0.00	280.28	0.00	0.00	0.00	0.00	0.00
Mixes	M11 UTM55NA	M12 TM20RA	M13 TM35RA	M14 TM55RA	M15 UTM20RA	M16 UTM35RA	M17 TM35RA	M18 TM.FA20NA	M19 TM.FA35NA	M20 TM.FA55NA
FA	0.00	0.00	0.00	0.00	0.00	0.00	0.00	30.00	52.50	82.50
MIBA	165.00	60.00	105.00	165.00	60.00	105.00	165.00	30.00	52.50	82.50
Cement	135.00	240.00	195.00	135.00	240.00	195.00	135.00	300.00	300.00	300.00
Water	160.55	196.13	195.99	195.82	196.13	195.99	195.82	160.77	160.77	160.77
Fine sand 0/1	297.34	302.22	301.34	300.17	302.22	301.34	300.17	303.39	303.39	303.39
Coarse sand 0/4	580.19	589.71	587.99	585.71	589.71	587.99	585.71	591.99	591.99	591.99
Sand-Gravel 2/5.6	100.34	0.00	0.00	0.00	0.00	0.00	0.00	102.38	102.38	102.38
Fine gravel 5.6/11.2	245.38	0.00	0.00	0.00	0.00	0.00	0.00	250.37	250.37	250.37
Coarse gravel 10/20	649.70	0.00	0.00	0.00	0.00	0.00	0.00	662.91	662.91	662.91
4 - 5.6	0.00	93.65	93.65	93.65	93.65	93.65	93.65	0.00	0.00	0.00
5.6 - 8	0.00	106.40	106.40	106.40	106.40	106.40	106.40	0.00	0.00	0.00
8 - 11.2	0.00	107.71	107.71	107.71	107.71	107.71	107.71	0.00	0.00	0.00
11.2 - 16	0.00	277.36	277.36	277.36	277.36	277.36	277.36	0.00	0.00	0.00
16 - 22.4	0.00	280.28	280.28	280.28	280.28	280.28	280.28	0.00	0.00	0.00

Different curing conditions were applied on the samples depending on the test type. In this study, the samples were placed in two chambers. The dry chamber had a relative humidity (RH) of $50 \pm 5\%$ and 22 ± 2 °C temperature. The wet chamber had a RH of $> 95\%$ and a temperature of 20 ± 2 °C.

3.3.4 Testing methods

Table 7 lists the testing methods to characterize the aggregates. According to EN 12620 and European Standards EN 933-1 (2000) and EN 933-2 (1999) as established in EN 12620 (2013), the particle size distribution was determined. To establish the final accurate results, this test was run three times for each type of aggregate. In order for the sieving to be regarded as genuine, it must be done in accordance with EN 12620 (2013) that the loss in percentage of the initial mass is less than 1%. The fineness module (FM) corresponds to the total of the accumulated percentages in standard sieves, divided by 100 when using the method provided in EN 12620 (2013).

Table 7 - Tests to determine the properties of aggregates

Aggregate properties	Test name	Standards
Geometrical	Determination of particle size distribution. Sieving method	EN 933-1 (2000)
		EN 933-2 (1999)
Mechanical and physical	Determination of the water content by drying in a ventilated oven	EN 1097-5 (2011)
	Determination of particle density	EN 1097-6 (2002)
	Determination of water absorption	EN 1097-6 (2002)

The particle density and water absorption tests were determined according to EN 1097-6 (2003). It was decided to apply tests on a sample set containing three specimens taken from each aggregate type throughout this experimental program. This would help eliminate inconsistency in the results if found. The results were achieved by measuring the average of the aforementioned three specimens. Considering that the method for determining density of the aggregate is based on the particles' size, it is suggested by the standard to use two procedures for 0.063-4 mm and 4-32.5 mm aggregates. This standard determines the procedures for limited ranges of particle sizes, which mandates separating the particles of the aggregate to obtain 0.063-4 mm and 4-31.5 mm samples. When calculating the three densities and WA of the sum, considering EN 1097-6 (2003), the following equations were used:

$$\rho_a = \frac{M_4}{(M_4 - (M_2 - M_3)) / \rho_w} \quad [8]$$

$$\rho_d = \frac{M_4}{(M_1 - (M_2 - M_3)) / \rho_w} \quad [9]$$

$$\rho_{ssd} = \frac{M_1}{(M_1 - M_2 - M_3) / \rho_w} \quad [10]$$

$$WA_{24} = \frac{100 \times (M_1 - M_4)}{M_4} \quad [11]$$

Where, ρ_a - apparent bulk density (kg/m^3); ρ_w - density of water (kg/m^3); ρ_d - oven-dried bulk density (kg/m^3); ρ_{ssd} - saturated surface dry bulk density (kg/m^3); WA_{24} - percentage of water absorption after 24 hours of immersion in water; M_1 - mass of saturated surface dry aggregate (g); M_2 - mass of pycnometer containing saturated aggregates and water (g); M_3 - mass of pycnometer filled with water only (g); M_4 - mass of oven-dried aggregates (g).

The hardened concrete specimens were tested for compressive strength (EN 12390-3, 2001). This test was conducted using $15 \text{ cm} \times 15 \text{ cm} \times 15 \text{ cm}$ cubic specimens in accordance with the standard. Three cubes were tested after 7, 28, 90 and 360 days. The samples were placed in the centre of the press (Type TONI PACT 3000 with the capacity of 3000 kN) after cleaning the machine's surfaces to avoid eccentricities. The load was applied at a constant speed of 13.5 kN/s until specimen failure (Figure 17). The compressive strength of the specimen was calculated in accordance with Eq. (6):

$$f_{cm,cube} \text{ (MPa)} = \frac{\text{Maximum force applied to the specimen (N)}}{\text{Cross section of the specimen (mm}^2\text{)}} \quad [6]$$



Figure 17 - Press machine (a) and sample reaching failure load (b)

3.4 Results and discussion

3.4.1 Composition of MIBA

In the first stage of grinding MIBA in the Los Angeles abrasion machine, a considerable amount of coarse particles was produced. As shown in Table 8 and Figure 18, particles had diameters between 2.4 mm and 10 mm, which made up more than 50% of the total mass of MIBA resulting from the process. This shows that the Los Angeles abrasion machine alone is ineffective at producing a cement-like powder as many of its components, tough brittle, are reasonably tough. Most of these particles were natural stones and ceramic (Figure 19).

Table 8 - Coarse fraction particle size distribution

Particle size (mm)	Mass (g)	Coarse non-magnetic/ Total (%)	Coarse magnetic/ Total (%)	All coarse/ Total (%)
> 10	1173.2	2.82	0.19	3.01
6.3 - 10	688.5	1.66	0.12	1.78
4 - 6.3	1309.8	3.15	0.17	3.32
2-4	1002.4	2.41	0.24	2.66
< 2	186.9	0.45	0.07	0.52
Total	4360.8	10.50	0.79	11.29

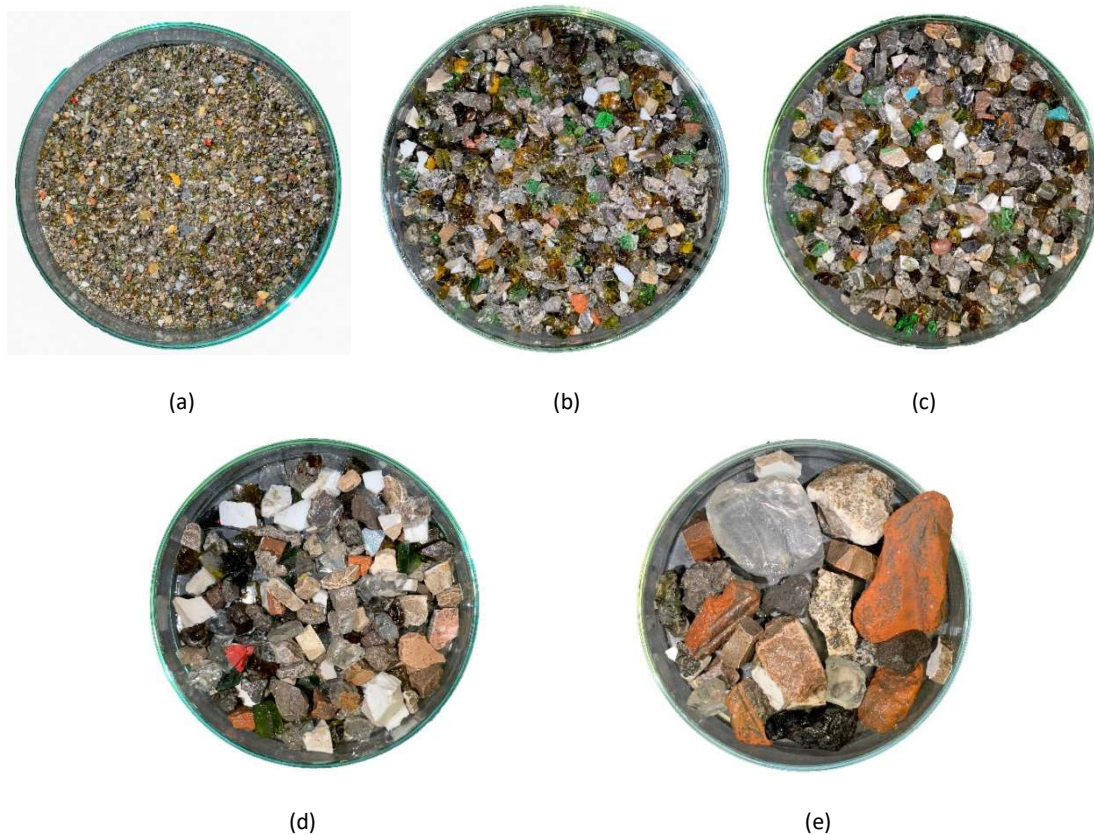


Figure 18 - Coarse fraction analysis: Under 2 mm (a); 2-4 mm (b); 4.6-3 mm (c); 6.3-10 mm (d); over 10 mm (e).

Table 9 - Fraction compositional analysis (size 2.2 - 4 mm)

Component	Amount in relation to total (%)	Type of materials
Colourless glass	31.1	Glass
Dark coloured mixture	1.3	Glass
Dark green/brown glass	36.2	Glass
Light coloured mixture	15.5	Quartz, calcite, aluminium, mullite, cristobalite, Kkyanite and anorthite
Light green glass	7.6	Glass
Magnetic	11.2	Magnetite, quartz, fayalite, augite aluminianaluminium and aluminium
Metallic mixture	1.4	Aluminium and mixed particles
Metals (copper)	2.3	Copper
Red ceramics	0.6	Quartz, amorphous, hematite
White ceramics	3.8	Quartz, mullite, anatase and calcite
Total		100.0



(a)



(b)



(c)



(d)



(e)



(f)



(g)



(h)



(i)



(j)

Figure 19 - Composition analysis: magnetic (a); colourless glass (b); dark green/brown glass (c); light green glass (d); light coloured mixture (e); white ceramics (f); red ceramics (g); dark coloured mixture (h); metallic mixture (i); metals (j)

After milling the samples for 90 minutes in the ball milling machine, additional coarse particles (1 mm) were removed after milling. This fraction includes white metallic flake-like particles, with high aluminium content, and low-density plastic particles. These particles were excluded for further applications, which were not considered for wet sieving analysis. The final product of milling was divided into different particle size distributions as shown in Table 10. The particle distribution of MIBA shows a similarity with the particle distribution of cement, as well as having similar fineness. These features infer an adequate specific surface area to allow chemical reactivity of MIBA when used as cement replacement. Figure 20 shows the sample after the milling process.

Table 10 - Fine product after 90 minutes milling (wet sieving analysis)

Sieve class	(g)	(%)	class	(%)
>300	1.83	0.70	<300	99.30
>150	5.60	2.15	<150	97.14
>75	86.91	33.43	<75	63.72
>38	48.88	18.80	<38	44.92
<38	116.79	44.92		
Total	260.00	100.00		

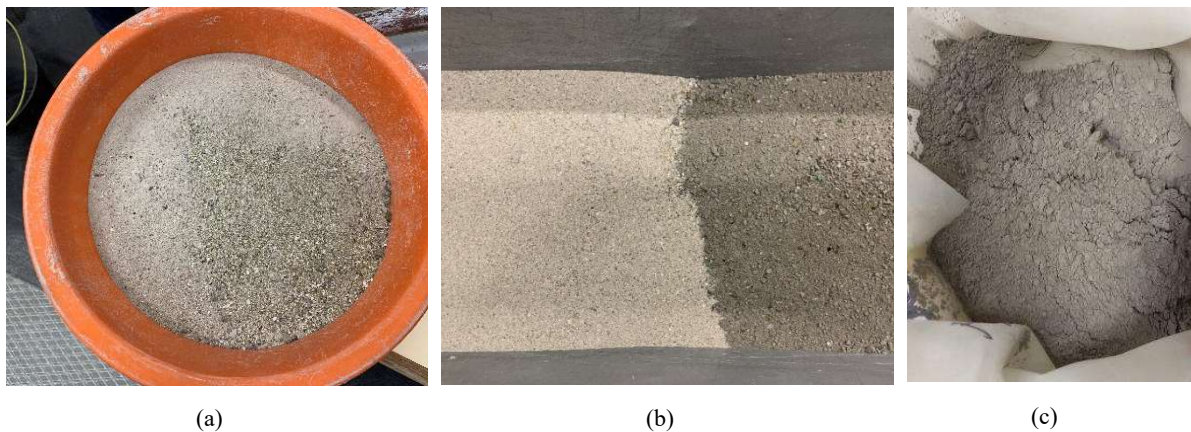


Figure 20 - Ground MIBA particles with a diameter greater than 4 mm (a); Comparison between ground MIBA with 4 mm diameter and MIBA after Los Angeles grinding (b); MIBA after the Los Angeles machine (c)

3.4.2 Aggregate characterization

According to the standard, the mass maintained on the bottom pan of the sieve column in different specimens should not differ by more than 1% of the initial weighed mass. The average particle size distribution results of fine and coarse sand, "rice grain," fine and coarse gravel are

shown in Table 11. As stated, each aggregate type was represented by three specimens. Furthermore, the findings reveal that the NA can be separated into two categories: fine and coarse aggregates. The first category, "fine aggregates," is made up primarily of particles with a diameter of less than 4 mm and is separated into fine and coarse sand. The second category, "coarse aggregate," is made up of "rice grain," fine and coarse gravel, with particles ranging in diameter from d_{min} to D_{max} , with D_{max} more than 4 mm.

Table 11 - Particle size distribution analysis of NA

Sieves (mm)	Fine sand	Coarse sand	"Rice grain"	Fine gravel	Coarse gravel
22.4	100.0	100.0	100.0	100.0	100.0
20.0	100.0	100.0	100.0	100.0	86.2
16.0	100.0	100.0	100.0	100.0	54.6
14.0	100.0	100.0	100.0	100.0	34.3
12.5	100.0	100.0	100.0	99.5	20.7
11.2	100.0	100.0	100.0	95.7	11.8
10.0	100.0	100.0	100.0	82.5	5.6
8.0	100.0	100.0	100.0	45.6	2.1
6.3	100.0	99.0	98.8	14.1	1.1
5.6	100.0	98.5	86.1	6.4	0.9
4.0	100.0	96.2	12.5	1.7	0.8
2.0	99.9	81.8	2.0	0.9	0.7
1.0	99.3	44.8	1.1	0.7	0.6
0.50	75.0	10.4	1.0	0.6	0.6
0.250	12.8	3.7	1.0	0.6	0.6
0.125	1.2	0.8	0.5	0.3	0.3
0.0625	0.1	0.3	0.3	0.3	0.2
D_{max}	1	4	5.6	11.2	22.4
d_{min}	0.125	0.250	2	6.3	10
Category					
FM	2.12	3.6	4.9	6.5	7.4

Fine aggregates, such as "fine and coarse sand," fall into the GF85 category, whereas coarse aggregates, such as "rice grain" and "fine and coarse gravel," fall into the GC85/20, Gc80/20, and Gc90/15 categories, according to EN 12620 (2008). Furthermore, according to the same standard, the maximum, minimum, and nominal sizes of fine aggregates are 1 mm, 0.125 mm, and 0/1 for fine sand, and 4.0 mm, 0.250 mm, and 0/4 mm for coarse sand. For coarse aggregates, the sizes are 5.6 mm, 2.0 mm, and 0/8 mm for "rice grain," 11.2 mm, 5.6 mm, and

4/11.2 mm for fine gravel, and 20 mm, 10 mm, and 4/22.4 mm for coarse gravel. The particle size distribution of both sand and gravel was well-graded and compact concrete can be made from them (Table 11). Fine and coarse sand had FMs of 2.12 and 3.6, respectively, according to Eq. (1). Rice grain, fine, and coarse gravel all had FM values of 4.9, 6.5, and 7.6, respectively. Figure 21 illustrates the resulting aggregate size distributions. The curves are the result of adding all sieve sizes (in logarithmic scale) and the percentage of cumulative passing material together (actual value). The graph indicates that the five aggregate types span the entire range of aggregates used in concrete compositions, ranging from 0 to 22.4 mm.

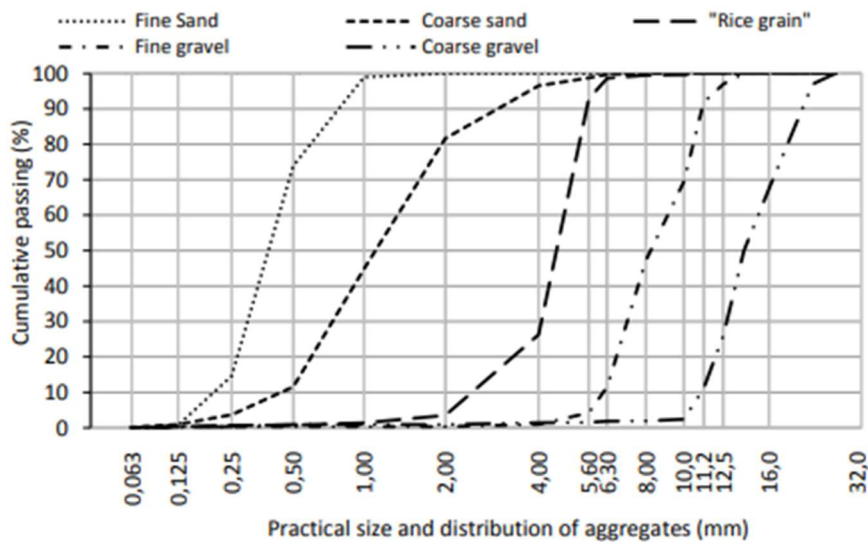


Figure 21 - Size distribution curves of NA

The apparent, oven-dried, and SSD particle densities of fine and coarse sands, "rice grain," fine and coarse gravels, and fine and coarse RCA are provided in Table 12. The oven-dried particle density is used to design the mix composition. As a result, it is crucial to compare the oven-dried particle density of this study to that of other investigations. The average oven-dried particle density of low and high FM sand collected from numerous investigations was $2,657 \text{ kg/m}^3$ and $2,613 \text{ kg/m}^3$, respectively. For fine and coarse sand, the oven dried particle density obtained from this investigation is extremely close to the values obtained from the literature review. The oven-dried particle density of the gravels in this investigation is within the stipulated range, similar to that of sand. The particle density of the NA was higher than that of the RCA, according to the literature. The coarse RCA particle density differs slightly.

The WA of NA and RCA obtained in this investigation, as well as the majority of studies, is

shown in Table 12. The WA of coarse RCA was found to be higher than that of coarse NA. This is because to their higher porosity (Evangelista and de Brito, 2007).

Table 12 - Particle density and WA of NA and RCA

Aggregates	ρ_a (g/cm ³)		ρ_{rd} (g/cm ³)		ρ_{ssd} (g/cm ³)		WA _{24 h} (%)	
	Current study	Literature review	Current study	Literature review	Current study	Literature review	Current study	Literature review
Fine sand	2.49		2.48	2.66	2.48	-	0.20	
Coarse sand	2.62	-	2.60	2.61	2.61	-	0.30	
Rice grain	2.68	-	2.61		2.64	-	1.00	
Fine gravel	2.69	-	2.55	2.55-2.81	2.59	-	1.50	0.3-1.67
Coarse gravel	2.69	-	2.60		2.63	-	1.30	
Coarse RCA	2.49	-	2.21	2.14-2.76	2.33	-	5.05	2.8-6.8

In this investigation, the WA of coarse RCA is quite similar to the values found in the literature review. Unlike RCA, NA had low values of WA, demonstrating its high quality and suitability for the manufacturing of high-performance concrete and allowing for better rheological control. The WA of coarse NA "gravels" was greater than that of fine NA sand. The w/b ratio is one of the most important parameters in concrete's performance. Water is required for cement hydration, which provides mechanical strength to concrete, but it must be dosed correctly. Too much water increases the porosity of concrete, lowering its mechanical performance and durability, while a lack of water causes incomplete cement hydration processes and a reduction in the workability of fresh concrete (Kurda, 2017). However, due to its modest size, the WA of NA may be overlooked.

Because the majority of RCA absorbs more water than NA, it is critical to collect the exact amount of water required during batch production. The WA was obtained for coarse RCA in this investigation at 24 hours according to EN 1097-6 and based on the method developed by Rodrigues et al. (2013). It was also decided that the mixing time of the concrete batches would be 10 minutes, because the concrete mix may leak if the water content thought to be absorbed by RCA is based on 24 hours.

3.4.3 Quantification of metallic aluminium in MIBA

Table 13 presents the results of the aluminium quantification test. Several iterations were tried in an attempt to minimize the amount of water and of NaOH that could guarantee an adequate release of H₂ gas. In these iterations, the quantities of water, NaOH and MIBA varied. The

latter was added in two different states: unprocessed, which means that the material was used as it was delivered from the MIBA treatment unit; and ground, following the steps mentioned previously to obtain a cement-like powder. The results suggest that, when in an unprocessed state, the amount of H₂ released is generally constant and around 85 ml for 15 g of MIBA. However, when using ground MIBA in the same conditions, the volume released doubled, suggesting that there were many unreacted aluminium particles. Further tests with molarities of 0.1 M for the ground sample showed insufficient release and that additional NaOH would be needed for adequate treatment.

Table 13 - Amount of H₂ gas released

Test	Quantity of water (ml)	Molarity (M)	Type of MIBA	MIBA (g)	Volume H ₂ (ml)	Q.AL (g/kg)	MIBA/W
1	800	0.25	Unprocessed	15	84	3.9	0.02
2	800	1	Unprocessed	15	80	3.7	0.02
3	800	1.5	Unprocessed	15	81	3.7	0.02
4	800	2.5	Unprocessed	15	78	3.6	0.02
5	800	10	Unprocessed	15	92	4.2	0.02
6	800	10	Ground	15	152	7.0	0.02
7	50	0.25	Unprocessed	25	121	3.3	0.50
8	50	0.1	Unprocessed	25	33	0.91	0.50
9	50	0	Unprocessed	25	0	0	0.50
10	50	0.1	Ground	25	87	2.4	0.50
11	50	0	Ground	25	0	0	0.50

After the trials presented in Table 13, more controlled testing was carried out on the ground MIBA treatment. Figure 22 presents the results of several trials using a solution with 50 ml water with a molarity of 0.25 (0.1 g NaOH). The ratio between MIBA and water was equal to 0.5 to avoid the use of excessive amounts of water for the treatment. At the beginning of the test, the period between readings was small because a large quantity of hydrogen was being released. After 6 hours, it was spaced by 3 hours until 15 hours of total test time and increased to 6 hours between readings until the end of the test (stabilization). Based on the five tests carried out to remove aluminium from MIBA, around 90% of the total H₂ release was observed in the first 24 h, and it took up to three days to observe stabilization. The higher molarity did not have a notable effect in more H₂ released, which indicates that a lower amount of NaOH can be used for the same results. Given the variability in the amount of H₂ released was different in each test, it is likely that there is a heterogeneous distribution of aluminium in the MIBA and that 25 g is unrepresentative of the actual material.

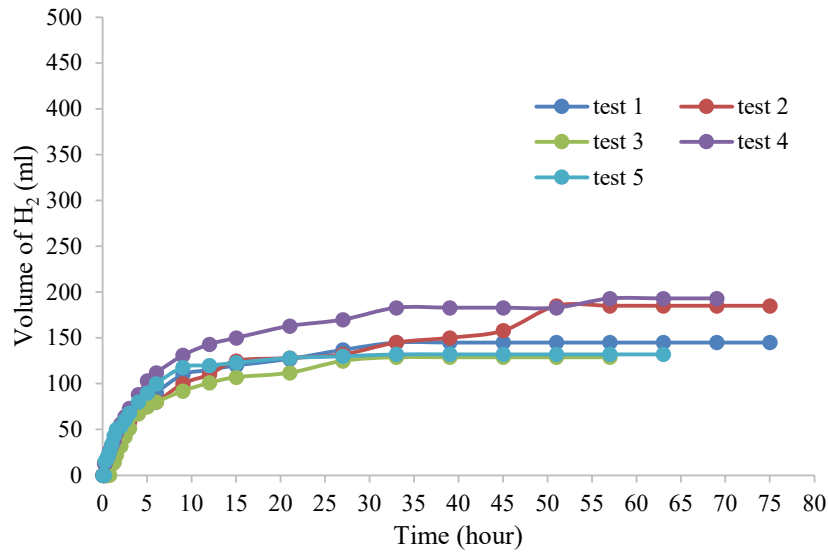


Figure 22 - Volume of H₂ released over the time in a solution with MIBA/W=0.5 and 25 g of MIBA

Figure 23 shows that the amount of hydrogen released by in a solution with MIBA/W =0.5 is similar to that released in a solution with a ratio of MIBA/W =1. This shows that a ratio MIBA/W=1 is applicable when treating MIBA as it can allow for a lower amount of water for the same results.

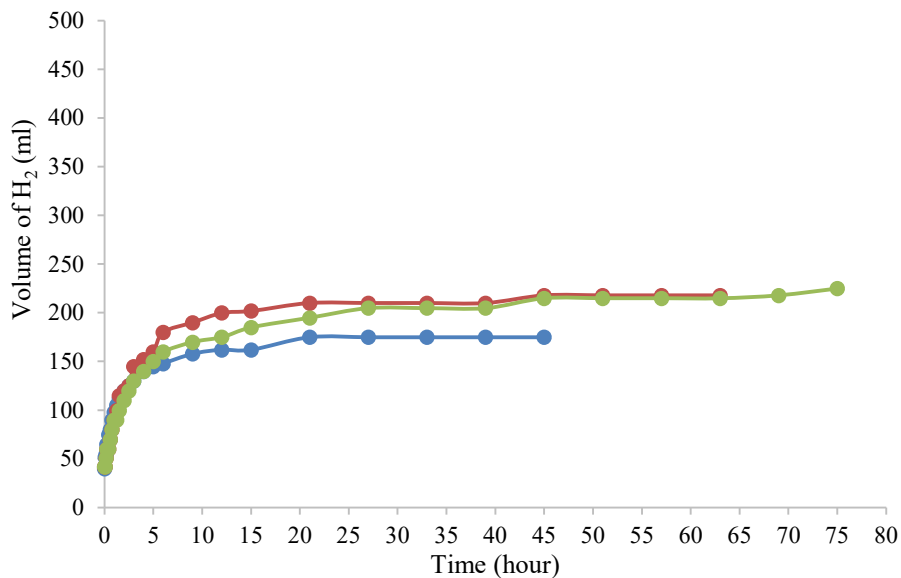


Figure 23 - Volume of H₂ released over the time in a solution with MIBA/W=1

Figure 24 presents the results of trials wherein the amount of MIBA and water were increased two-fold to check whether the treatment process was not affected by the quantity of MIBA. Thus, for a MIBA/W ratio of 1, two groups of tests were conducted for quantities of MIBA

equivalent to 25 g and 50 g. The results were similar, which suggests that the treatment process exhibits the same behaviour regardless of the amount of MIBA treated.

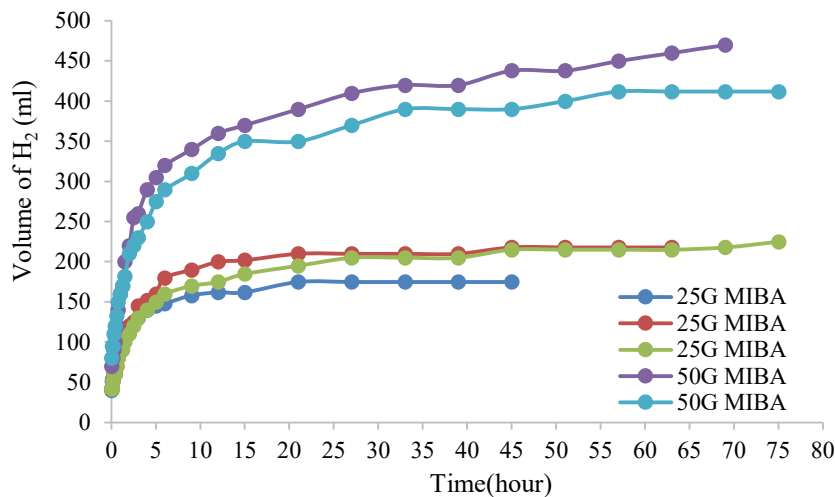


Figure 24 - Volume of H₂ released over the time in a solution with MIBA/W=1 using 25g / 50g of MIBA

3.4.4 Compressive strength

The compressive strength of concrete is seen as one of the most influential parameters for determining the loading level that can be applied to a structural member. In addition, it gives an indication of most of the features of concrete. The compressive strength of RCA concrete mixes may depend on the RCA incorporation level, concrete age, incorporated admixtures and additions, and quality of the source material RCA (Silva et al., 2015). The main factor affecting the performance of this precursor is the existence of metallic aluminium (Al), which leads to damaging expansive reactions and an increase in porosity due to H₂ gas generation stemming from the response with the alkaline activator (Kurda et al., 2020). Table 14 shows the results of compressive strength for 20 mixes for 7, 28 and 91 days.

Incorporating MIBA in concrete mixes is detrimental in terms of compressive strength as shown in Figure 25 and Figure 26. The development of compressive strength for FA is higher than MIBA, regardless of being treated. The difference between the strength of conventional concrete and concrete with FA decreased over time, as a result of the relatively slower pozzolanic reactions between FA and the cement's hydration products (Silva and de Brito, 2013). Furthermore, incorporating FA in concrete mixes is harmful to compressive strength, more precisely at younger

ages. After 28 days, the amount of strength development of the treated MIBA as well as untreated MIBA concrete is significantly lower than that of the mixes with FA for older ages. Moreover, the compressive strength development of treated MIBA concrete mixes is higher than that of untreated MIBA concrete mixes. This is caused by the treatment process of MIBA, which eliminates the presence of aluminium within MIBA. That in turn solves the problems of the air bubbles caused by aluminium, sequentially improving the compressive strength.

Table 14 - Compressive strength of test specimens at various ages

FA (%)	UT.MIBA (%)	T.MIBA (%)	Coarse RCA (%)	7		28		91	
				fcm, cube (MPa)	fcm, cube at 7d/fcm, cube at 28d	fcm, cube (MPa)	fcm, cube at 28d/fcm, cube at 28d	fcm, cube (MPa)	fcm, cube at 90d/fcm, cube at 28d
0	0	0	0	40.2	0.82	48.74	1	50	1.03
20	0	0	0	25.67	0.73	35.37	1	41.53	1.17
35	0	0	0	21.5	0.74	29	1	39.5	1.36
55	0	0	0	12.5	0.68	18.43	1	28.63	1.55
0	0	20	0	22.43	0.76	29.53	1	32.77	1.11
0	0	35	0	13.5	0.78	17.37	1	20.6	1.19
0	0	55	0	2.3	0.56	4.13	1	4.53	0.14
0	0	0	100	36.43	0.85	43.07	1	46.83	1.09
0	0	20	100	18.43	0.81	22.87	1	27.2	1.19
0	0	35	100	9.2	0.77	12	1	14.53	1.21
0	0	55	100	3.2	0.74	4.3	1	5.77	1.34
0	20	0	0	17.63	0.85	20.70	1	25.97	1.25
0	35	0	0	9.43	0.86	10.97	1	15.23	1.39
0	55	0	0	4.9	0.73	6.73	1	8.77	1.30
0	20	0	100	17.53	0.94	18.67	1	22.57	1.21
0	35	0	100	8.90	0.75	11.93	1	14.17	1.19
0	55	0	100	4.03	0.70	5.77	1	7.77	1.35
10	0	10	0	23.5	0.83	28.4	1	38.17	1.34
17.5	0	17.5	0	15.6	0.76	20.53	1	25.3	1.23
27.5	0	27.5	0	7.87	0.68	11.5	1	15.9	1.38

The incorporation of RCA in concrete mixes has harmful effects in terms of compressive strength. Figure 25 illustrates how incorporating 100% coarse RCA is remarkably detrimental for MIBA concrete mixes due to the presence of lower-density residual cement mortar attached to the RA particles, leading to high water absorption (Kurda et al., 2020). However, the results

of incorporating either coarse RCA or MIBA alone have less more damaging effect compared to concrete mixes with both compounds incorporated. In general, the use of 100% RCA with MIBA has a slightly negative effect.

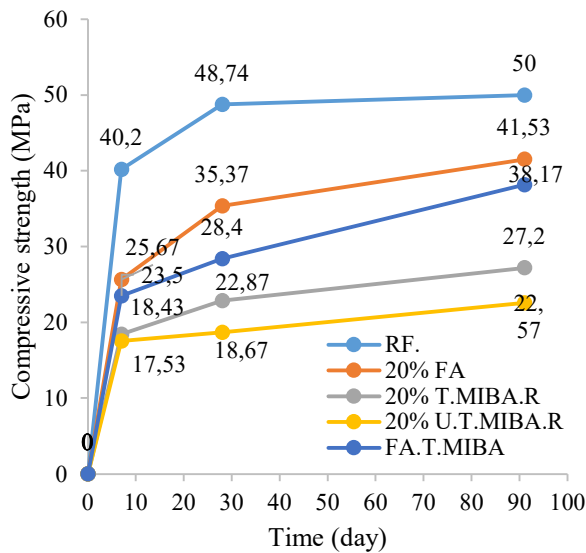


Figure 25 - Compressive strength for RCA mixes after 28 days

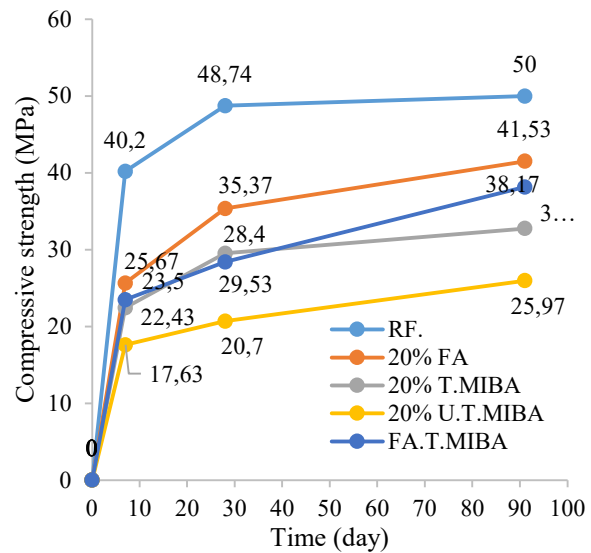


Figure 26 - Compressive strength for NA mixes after 28 days

The compressive strength is significantly affected by the MIBA incorporation ratio and the aggregates NA and RCA. Figure 27 and Figure 28 shows the relationship between the compressive strength of concrete specimens and the replacement ratio of MIBA either with NA or RCA, respectively. There is a decline in the values of compressive strength as incorporation ratios increase. The treated MIBA with RCA reached the lowest value of 4.3 MPa.

Predictably, there is an inverse proportion between the rise of incorporation ratios of MIBA and the compressive strength of concrete as shown in the aforementioned figures. European standards (EN 197-1, 2000) restrict the incorporation level of supplementary material up to 55% of cement mass because higher incorporation leads to considerable decline in performance. This was observed in this study, where mixes that have a 55% of MIBA were the worst whether treated or untreated MIBA were used. Most of MIBA is likely acting as a filler rather than as a binder, which damages the microstructure of concrete. On the other hand, the results show that, after 90 days, the strength of concrete significantly decreased when incorporating 20% of MIBA, with a greater decrease for higher incorporating ratios of MIBA, and this is

another reason why the European standard recommends a maximum replacement of cement mass with FA of 55% (Kurda et al., 2020). Based on the two aforementioned figures, treated MIBA has better values, for low incorporation ratios, in terms of compressive strength when compared to untreated MIBA, with both treated and untreated MIBA achieving approximately similar values. Figure 26 shows that the mix that has both FA and MIBA (20%) acted better than those that have only treated MIBA and worse than the mix of only FA.

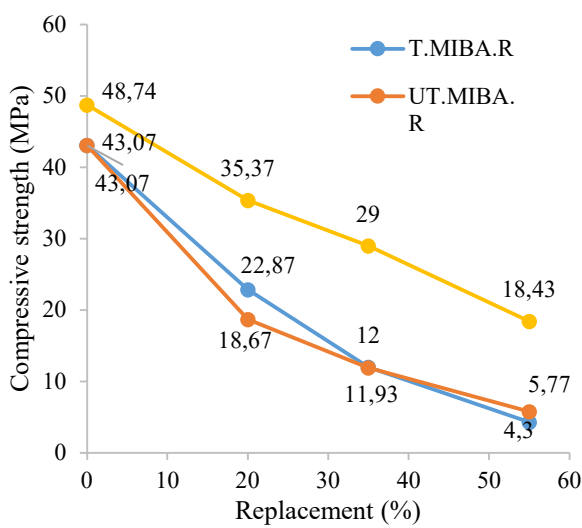


Figure 27 - Compressive strength for RCA mixes for multiple incorporation ratios

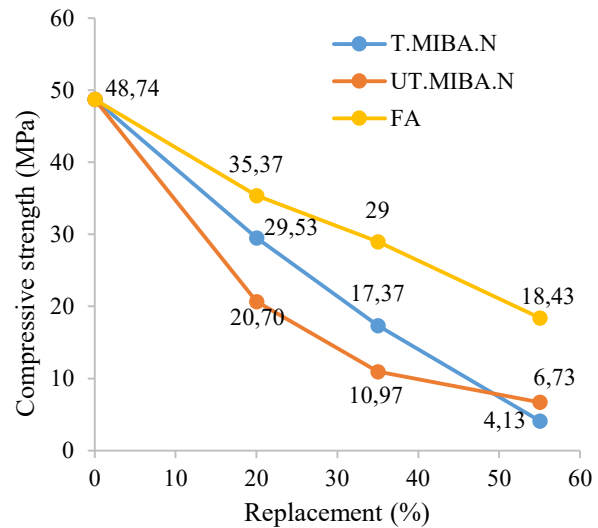


Figure 28 - Compressive strength for NA mixes for multiple incorporation ratios

4 Conclusions

Based on the process of preparing MIBA for the mixes, a fairly large amount of organic and plastic materials is already present within MIBA before the grinding process. This indicates the poor quality of MIBA and suggests the necessity of more controlled waste incineration in order to produce MIBA. The presence of these organic and plastic components poses a threat to the workability and physical state of concrete containing MIBA. The physical study of MIBA also showed a tremendous amount of glass, which is an important trait indicating the material's reactivity.

The experiments carried out showed that the solution with a molarity of 0.25 achieved the best ratio of aluminium removal from MIBA. Additionally, it can be considered as the more sustainable iteration due to the small amount of sodium hydroxide used. Grinding MIBA, obviously, led to best results due to the increase in the number of interacting particles of aluminium

with NaOH. Moreover, when treating MIBA, the time needed for the process of treating decreases as the molarity increases, which indicates an inverse relationship between the time of processing and the molarity.

There was an overall decline in performance with the addition of MIBA when compared with mixes made with the same amount of FA. However, the decline was less noticeable when a treated MIBA was added. The treatment led to a considerable release of H_2 from the oxidization of aluminium. This prevented the formation of H_2 bubbles in concrete in the fresh state and, consequently, the expansion of specimens during their setting. Still, it is clear that MIBA is not as reactive as FA, thereby leading to lower amount of pozzolanic reactions. Future trials on the concrete mixes over a more extended period of time will allow evaluating how well MIBA behaves as a mineral addition in concrete.

References

Alderete M, Joseph M, Van den Heede P, Matthys S and De Belie N (2021). Effective and sustainable use of municipal solid waste incineration bottom ash in concrete regarding strength and durability. *Resources, Conservation and Recycling* 167: 105356.

ASTM International (2012) ASTM C618-12a Standard specification for coal Fly Ash and raw or 13 calcined natural pozzolan for use in concrete. 12a:5.

CSA-A23 (1982). Concrete materials and methods of concrete construction/test methods and standard practices for concrete. Canada, Canadian Standards Association (CSA).

EN 1097-2 (2010). Tests for mechanical and physical properties of aggregates. Methods for the determination of resistance to fragmentation, Brussels, Belgium, CEN: 38.

EN 1097-3 (1998). Tests for mechanical and physical properties of aggregates. Determination of loose bulk density and voids, Brussels, Belgium: CEN: 10.

EN 1097-3 (1998). Tests for mechanical and physical properties of aggregates. Determination of loose bulk density and voids, Brussels, Belgium: CEN: 10.

EN 1097-6 (2013). Tests for mechanical and physical properties of aggregates. Determination of particle density and water absorption, Brussels, Belgium: CEN: 54.

EN 12350-2 (2009). Testing fresh concrete. Slump-test, Brussels, Belgium, CEN: 12.

EN 12350-6 (2009). Testing fresh concrete. Density, Brussels, Belgium, CEN: 14.

EN 12350-7 (2009). Testing fresh concrete. Air content. Pressure methods, CEN.

EN 12390-3 (2009). Testing hardened concrete. Compressive strength of test specimens, Brussels, Belgium: CEN: 22.

EN 12390-6 (2009). Testing hardened concrete. Tensile splitting strength of test specimens, CEN: 14.

EN 12390-7 (2009). Testing hardened concrete. Density of hardened concrete, CEN: 14.

EN 12457/1-4 (2002). Comité Européen de Normalisation. Characterization of waste. Leaching - compliance test for leaching of granular waste materials and sludges. Brussels, Belgium, CEN.

EN 12504-4 (2004). Testing concrete. Determination of ultrasonic pulse velocity, CEN.

EN 12620 (2008). Aggregates for concrete, CEN. 60.

EN 12620 (2013). Aggregates for concrete, CEN, Brussels, Belgium:56.

EN 15804 (2012). Sustainability of construction works - Environmental product declarations - Core rules for the

EN 197-1 (2000). Cement. Composition, specifications and conformity criteria for common cements, Brussels, Belgium, CEN: 50.

EN 1992-1-1 (2004). Eurocode 2: Design of concrete structures. General rules and rules for buildings, CEN: 230.

EN 206-1 (2000). Concrete - Part 1: Specification, performance, production and conformity, CEN, Brussels, Belgium:72.

Evangelista L and de Brito J (2007). Mechanical behaviour of concrete made with fine recycled concrete aggregates. Cement and Concrete Composites 29(5): 397-401.

India: 905-918.

Kurda R (2017). Sustainable development of cement-based materials: Application to recycled aggregates concrete. Instituto Superior Técnico, Universidade Técnico de Lisboa. Portugal. PhD thesis in civil Engineering.

Kurda R, Silva R and de Brito J (2020). Incorporation of alkali-activated municipal solid waste incinerator bottom ash in mortar and concrete: A critical review. Materials (Basel) 13(15): 3428.

NP EN 1097-5 (2011) - Tests for mechanical and physical properties of aggregates. Part 5: Determination of moisture content (in Portuguese), IPQ, Lisbon.

NP EN 1097-6 (2003) - Tests for mechanical and physical properties of aggregates: Determination of density and water absorption (in Portuguese), IPQ, Lisbon.

NP EN 1097-6 (2003) - Tests for mechanical and physical properties of aggregates. Part 6: Determination of density and water absorption (in Portuguese), IPQ, Lisbon.

NP EN 933-1 (2000) - Tests for geometrical properties of aggregates. Part 1: Particle size distribution. Sieving method (in Portuguese), IPQ, Lisbon.

NP EN 933-2 (1999), NP EN 933-2, Tests for geometrical properties of aggregates. Part 2: Determination of particle size distribution. Test sieves, nominal size of apertures, IPQ, Lisbon product category of construction products. Brussels, Belgium, CEN.

Rodrigues F, Evangelista L and de Brito J (2013). A new method to determine the density and water absorption of fine recycled aggregates. *Materials Research* 16(5): 1045-1051.

Silva P and de Brito J (2013). Experimental study on chloride migration coefficients of SCC with binary and ternary mixtures of fly ash and limestone filler. UKIERI concrete congress - Innovations in concrete construction in

Silva R (2015). Use of recycled aggregates from construction and demolition wastes in the production of structural concrete. Instituto Superior Técnico, Universidade de Lisboa. Portugal. PhD Thesis in Civil Engineering: 274.

Lisboa, 25th September, 2022

Authors

Salem Anezami

PhD Candidate

Rawaz Kurda

PhD Researcher

Rui Vasco Silva

PhD Researcher

Jorge de Brito

Full Professor